Available online at https://sanad.iau.ir/journal/jrors

Publisher: Yazd Branch, Islamic Azad University

Journal of Radar and Optical Remote Sensing and GIS

ISSN: ***2645-5161***

Soil moisture extraction using Microwave Imagery (Case Study: Behshahr, Mazandaran)

Abolfazl Rahimabadi [a]✉

[a] *Department of GIS & RS, Yazd Branch, Islamic Azad University, Yazd, Iran*

ARTICLEINFO

Research Type:
Research article

Article history:
Received 15 January 2024
Received in revised form 01 February 2024
Accepted 07 April 2024
Published online 15 May, 2024

Keywords:
Backscatter Coefficient;
Soil Moisture;
SAR;
Sentinel-1;

ABSTRACT

Objective: Estimate the large part of the soil surface to calculate its moisture is very important for agriculture since it would improve food security. In current study, four radar images of Sentinel-1 are employed to observe soil moisture in Miyankale Peninsula where is located in Behshahr, Mazandaran province.
Methods: These data are collected since 1394 until 1395 in both VV and VH polarization while imagery mode is Global mode. Soil texture, vegetation disturbs microwaves responses therefore the images are processed to eradicate vegetation effect, then backscatter coefficient calculated.
Results: These backscatters connect to statistical information gathered by field sampling (hygrometer device) to determine volumetric soil moisture in Miyankale Peninsula. The results show 0.79 for R^2 (coefficient of determination) between volumetric moisture and backscatter; 0.62 for R^2, between vegetation and backscatter, which confirm the vegetation effect on detecting moisture of soil.
Conclusion: This effect is removed from backscatter. In this study, Global mode in SAR data is appropriate for spares vegetation areas.

1. Introduction

One of the soil parameters that would affect other parameters is moisture thus the focus of this research is calculating the amount of moisture of the soil. Although soil moisture has been measured through other researches, this research proposed then examined a novel method to do so. Applying satellite data to measure the amount of moisture in the soil is a new method as least in Iran. There were a few radars practical examinations which dedicated to soil parameters such as moisture. Among various satellite data, radar data is an appropriate data to extract the moisture percent in the soil. In other words, radar spectrum is more capable than other electromagnetic spectrum to detect moisture in the soil. Therefore, radar satellite has been chosen to detect the soil moisture. The Sentinel-1 has a sensor, SAR named, which produces and sends radar waves to the earth then receives the backscatter returned from the earth features (Thain, et al, 2011). This current research chose the new method of radar imagery by downloading several images of the Sentinel-1, to calculate the soil moisture. Determination of soil moisture is important for agriculture products (Potin, et al, 2011).
From now on, it will be explained the method employed to extract soil moisture. The images were processed to map soil moisture parameters of the case study to determine the amount of moisture in each image.

* *Corresponding author.* Tel.: 0098-9359405245.
E-mail address: rahimabadi_abolfazl@yahoo.com, ORCID: 0000-0003-xxxx-9443
Peer review under responsibility of Yazd Branch, Islamic Azad University

DOI: https://doi.org/10.30495/xxxxx.2023.1963135.xxxx

An algorithm is needed to be investigated and implemented in order to retrieve soil surface parameters. Soil parameters such as moisture and roughness are used in various fields. SAR[1] capability to measure soil parameters is known for more than 30 years now however, scientists are still searching for appropriate sensors and applicable algorithms to restore soil parameters (Mirmazlumi, 1393, p. 43). For instance, European Space Agency (ESA) scientists used radar wavelength with the SMOS[2] in order to measure two variables: soil moisture and salinity of the oceans (Mecklenburg, 2015, p. 4). Radar images have two sections included power and phase (backscatter), which are used to determine the moisture content of the soil. Humidity is expected to be directly related to power. This research modeled the changes in radar images. Radar wavelengths are able to detect the difference content of the moisture in soil. Finally, the results obtained with these wavelengths will be analyzed and mapped in the case study of Miyankale.

1.1. Soil surface parameters

Generally, soil surface parameters can be subdivided into three categories:

1. Surface roughness parameters: These parameters include: the distribution of ground targets, surface profile height and autocorrelation function and surface roughness criteria.
2. Soil Properties: surface roughness, water capacity, depth of penetration and macro-level structure are included in this category.
3. Vegetation characteristics: The vegetation structure and geometry of the plant, along with the water capacity of the plant, are the most important parameters of this category (Mirmaslomi, 1393, p. 56).

1.2. Research literature

Ebrahim Babayan et al. (1392) used ASAR images to estimate soil moisture content and also TDR humidifier to validate the data. It is concluded that the GM mode of ASAR images is more appropriate to be used in semi-arid and undercoats conditions to estimate soil moisture content. Dr. Entekhabi's methodology was developed in 1994. Dual soil moisture model and heat loss model are employed to measure moisture and surface temperature. These measurements processed and used to estimate the moisture and then generalized it to the depths of surface. Foson Balik et al. (2008) used the backscatter waves of ASAR, PALSAR and RADARSAT-1 radar sensors, to measure soil moisture 86%, 76% and 81%, respectively. Balik compared different polarizations of three sensors and concluded that in spite of better spatial resolution 30*30 meter of ASAR image, the results are almost the same in the study area Izmir of Turkey. Also, Saloni et al. (2008) compared the accuracy of ASAR images (band C, HH and VV polarization), RADARSAT-1 and PALSAR (L band, HH polarization) to estimate soil moisture content in agricultural land in western Turkey. According to their results, the relationship between soil moisture content and backscatter coefficient of soil was R2 = 0.77, 0.81 and 0.86, respectively. In another study, Brocka et al. (2011) used the passive microwave data of the AMSR-E sensor of Aqua satellite and ASCAT sensor of MetOP Satellite to measure moisture content of the soil surface, with correlation coefficients (R) 0.71 and 62.2, respectively. Baghdadi et al. (2012) estimated the soil moisture content in vegetation-free conditions with a precision of 3% using the TERRASAR-X test data. Lyons and Verhoest (2012) detected the correlation between RADARSAT-2 data in HH and VV polarizations. The IEM[3] model estimated the soil moisture content, with the RMSE equal to 0.04 (cubic centimetre per cubic centimetre). Kulas et al. (2016), found improvements in detecting soil moisture in the ranges of 5 to 19 percent. In an investigation which they worked on microwave satellite data for the assessment of soil moisture, it was found that if active satellite (ASCAT) and passive (AMSR) data were used complementarily, a significant improvement would be obtained. Lyons et al.

1- Synthetic aperture radar
2- The Soil Moisture and Ocean Salinity
3- Integrated ecosystem model

(2017) did the same study by two observations. Both active radar (ASCAT) and passive (SMOS) considered to observe backscatter coefficient and lighting temperature. Lyons found out that combining these parameters would estimate the soil moisture in depth of 0-10 cm with a great accuracy of 0.548.

2. Materials and Methods

The research based on two types of data; field data and satellite data. The field data were going to examined soil in the case study in order to measure the amount of soil moisture. These field measurements were necessary to be done to compare with the moisture obtained by radar images. In further section it would be cleared the relationship between field data and satellite data. First of all, the case study has been introduced.

2.1. Study area

The Behshahr city is located in the mountainous foothills of Alborz Mountains with two mountainous and plain areas. It extends from 36 degrees, 45 minutes to 36 degrees and 88 minutes longitude, and 53 degrees and 21 minutes to 54 degrees 13 minutes latitudes. Miyankale Peninsula is located in this city as a plain district next to the Caspian Sea. The Miyankale is a narrow Peninsula were reached to the Caspian Sea from the north, and reached to the narrow, shallow Gorgan Gulf from the south. It restricted by Raghmarz wetland from the west and narrow strait of less than one kilometre in the neighbouring port of Turkmen from the east.
The area of Miyankale is a unique area about 68 thousand hectares. The average height of this area is 30 meters below the sea level, and its annual rainfall is 717 mm. Miyankale is located in a warm, humid climate. The terrestrial ecosystem consists of sandy hills of the Pomegranate trees, berry bushes, Sail bushes and grassland region. These various vegetation areas are not uniform and are dense in some hectares but thin in others.

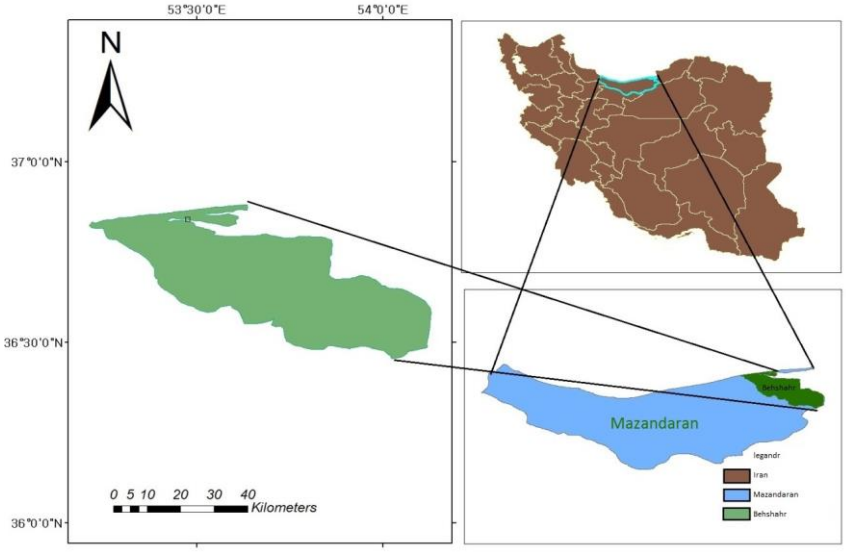

Fig. 1. The case study of Behshahr

2.2. Field data

Besides processing satellite data, the field data were collected in 1m2 kilometer area is considered to be checked in soil moisture. The observed moisture content was calculated in depth (1-10) centimeters. The forty samples were obtained in different location. The samples were kept in specific metal dish in order to transfer to the soil laboratory. The soil laboratory measured the percentage of moisture content. The location of each sample point was recorded by the GPS device Fig. 2. Another point that has to be noticed is the different types of sampling. The soil differed from sand to gravel and vegetation types in sampling positions varied from thin to dense grass to a height of 10 centimeters. It should be considered that, during software processing, the effect of vegetation would be removed.

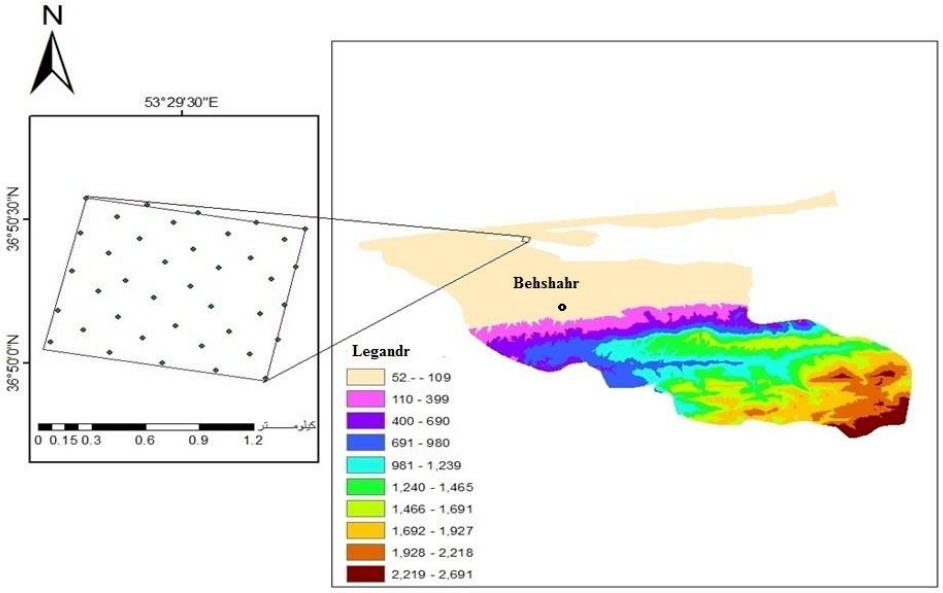

Fig. 2. DEM of Behshahr; (writers)

2.3. Satellite data

Two satellite were considered to employ their images; LANDSAT-8 and SENTINEL-1. As long as SENTINEL-1received all the radar backscatter from the ground, it needed to delete the vegetation backscatter. The impact of vegetation had to be eradicated then the radar image processed to measure the soil moisture. The NDVI is a vegetation index which obtained by LANDSAT-8. Three images of Landsat 8 were downloaded in approximately the same date of the radar images were obtained. LANDSAT-8 images were pre-processed then processed to calculate the vegetation density in the case study of Miyankale Peninsula. Then NDVI index needed to be calculated in order to measure, the LAI equation (1):

$$LAI = 0.57 * \exp(2.33 * NDVI)) \quad (1)$$

3. Methodology

The European Space Agency is an open source to get the Sentinel-1 images. These are high resolution images with a large frame size of 40,000 pixels * 40,000 pixels. First of all orbital correction is exerted

to the image. There are two types of correction files, POEORB, RESORB. The RESORB file is easier to access rather than another file. It could be downloaded in less than a day; however, the POEORB orbit took longer period to be available but it was more accurate. Thus, the POEORB file was used in this research. The next step was to remove the thermal noise and then the image calibrated by Sigma0 band. As long as the pixel size is half of the SAR image resolution, the image's speckle was removed by making multilook of the image.
Each pixel is the result of a total of backscatter to the satellite, and each backscatter has a different phase. Therefore, the interference of these waves causes the formation of dark or bright spots in the final image. This created noise, such as salt and pepper, is sprayed on images; it is unavoidable error in coherent systems Fig. 3.
For each pixel, γ (x, r) is equal to the sum of the backscatter (2):

$$|u(x_0, r_0)| = |\gamma(x_0, r_0) * u_0(x, r)| = |\Sigma\, \gamma_i(x_0, r_0) * u_0(x, r)| \quad (2)$$

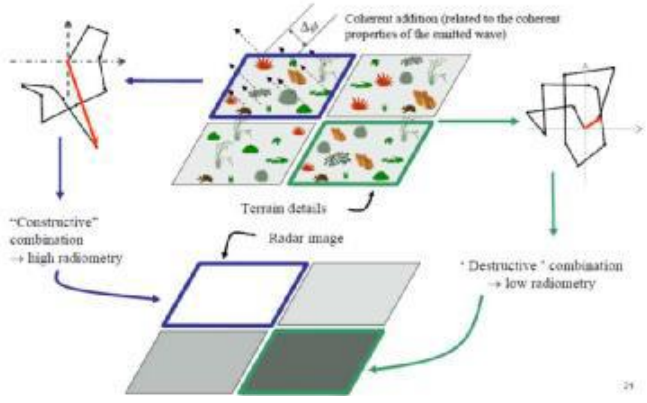

Fig. 3. Backscatter of each pixel. Source: Mincla, 2016

The effects of speckles on the image degraded image quality so the interpretation became more difficult. According to the Fig. 4 As the backscatter increased, the speckle would increase too.

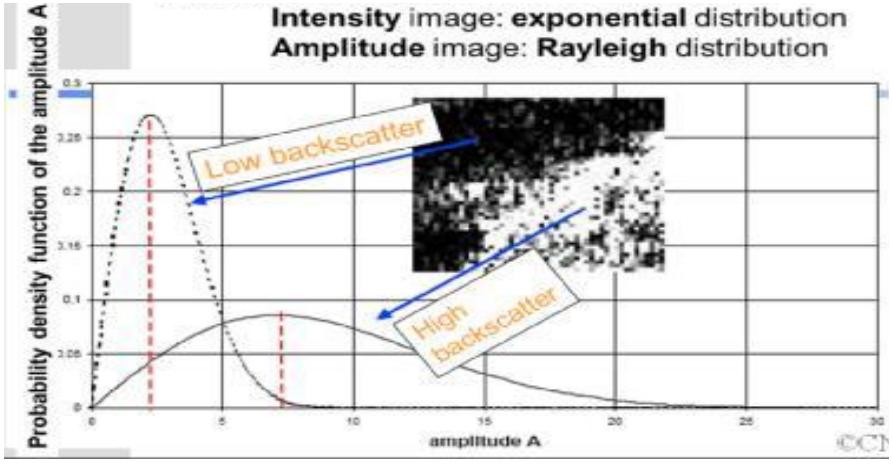

Fig. 4. The relationship between word and image and post back. Source: Mincla, 2016

In this paper, the Moody's filter was used (Babayan, 1392: 613) to remove speckles. As the multi look increased, the probability distribution function became narrowed. The narrow function is corresponded the speckle reduction in the image (Mincla, 2016). The speckle of the images would remove using different date of imagery of the same place. In other word, various images of the case study in different time are the solution for detecting speckles. In the next procedure geometric correction, georeferenced and normalization of the slope of the area was exerted. The slope is corrected by the Band Math operator shown in quotation (3). Now the sigma zero[4](σ °) of the region is calculated by multiplying backscatter of the reference ellipse to the sinusoidal fraction Fig. 6. The θ_{DEM} is the angle of the radar wave with the digital elevation model and θ_{ELL} is the angle of the wave with the reference ellipse.

$$\text{Area: } \sigma^{\circ}\text{Norm} = \sigma^{\circ}\text{Ellipsoid} * \frac{\text{Sin}\theta\text{DEM}}{\text{Sin}\theta\text{Ell.}} \qquad (3)$$

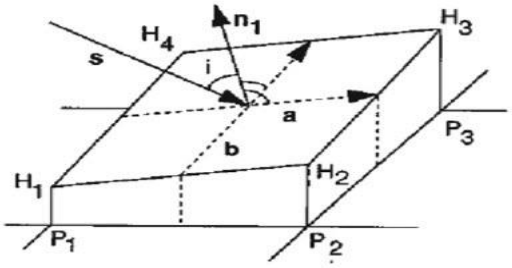

Fig. 5. The reflection relation with the gradient of its reflection surface. Source: Mincla, 2016

The radar image is composed of phase or power that should be converted to a user-friendly image. How to display the Sentinel image depended on the received geometry. After processing the image data in Fig. 6, it was time to estimate the moisture content and the backscatter relationship with the moisture content of the studied area and vegetation density.

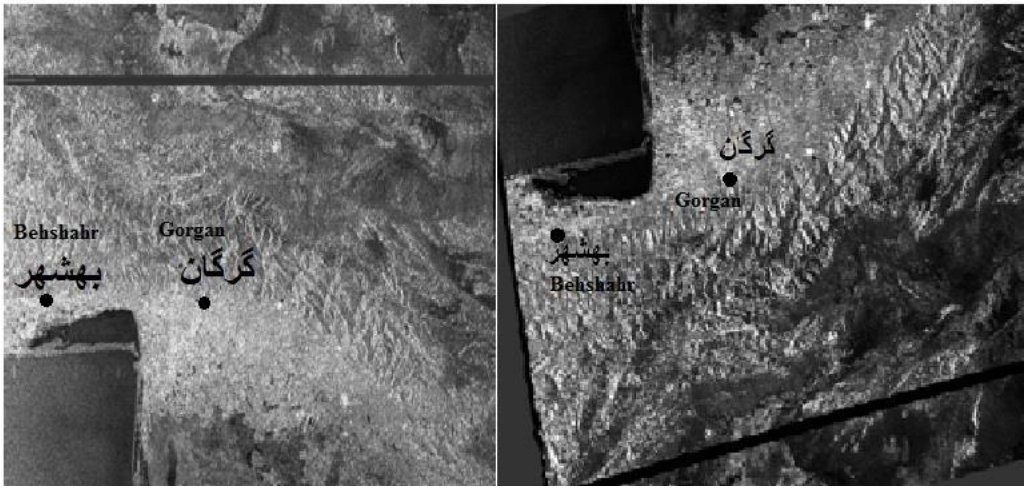

Fig. 6. The right image is the final processing. Source: Writers

The backscatter of the earth surface was obtained using equation (4). Where σs° soil backscatter and

4- Sigma Nought

σdv° plants backscatter, and also σ int ° is the backscatter of the plant and soil. The plant backscatter is derived of these equations (5) and (6) where τ2 is the portion of light which transferred of the vegetation surface and LAI is the leaf area index. The angle θ is declination of the sensor (Moren, 2005: 8).

$$\sigma^{\circ} = \tau\sigma_{s}^{\circ} + \sigma_{dv}^{\circ} + \sigma_{int}^{\circ} \quad (4)$$

$$\tau^{2} = \exp(-2\mathrm{LAIsec}\theta) \quad (5)$$

$$\sigma_{dv}^{\circ} = \mathrm{LAIcos}\theta(1-\tau^{2}) \quad (6)$$

4. Results and discussion

The coefficient of determination, denoted R^2 "R squared", is used to compare independent variable(s). The research had two types of data were also independent; first group were field measurements and the second one was images calculation. It should be considered these two types of data were prepared independently in order to compare. The calculation of R^2 coefficient is an appropriate method to compare these data. The research chose this method to examine the correctness of moisture percent extracted form SAR imagery. Since the field moisture were measured correctly, the R^2 coefficient determined the correctness of moisture measurements on SAR images. In other words, R^2 is capable of determination of SAR imagery whether it detected the soil moisture in a correct way or not. The coefficient of determination ranges from 0 to 1. As the R^2 value became closer to 1, the moisture obtained from SAR images was confirmed.

4.1. Comparison of surface reflection coefficients and observation of humidity

The coefficient (R^2) is 0.82, 0.82, 0.78, 0.72, and 0.81 for different time periods were obtained as shown in Table (1). The difference between these two variables can be due to the backscatter received by the sensor, which included the polarization and the soil's types (Altis, 1996, p. 655).
The coefficient (R^2) obtained from the diagrams indicated that the coefficient of determination differed from 0.72 to 0.82 due to the moisture content and backscatter in different time series. The least amount of R^2 is for VH polarization. Also, for the coefficient of determination, different results were obtained, which will be described below.

Table 1: Results of RMSE and R2 coefficient and moisture variables observed in different time series

R2	RMSE	Polarization	Date
0.82	0.35	VV	11/21/2015
0.82	1.06	VV	5/1/2016
0.78	1.49	VV	6/5/2016
0.72	1.75	VH	6/5/2016
0.81	0.68	VV	9/22/2016

4.2. Comparison of backscatter coefficient with Vegetation (NDVI)

The relationship between vegetation and wavelength is important because, in detecting soil moisture, the wavelength must be passed through vegetation as the main obstacle and reached to the soil. According to Babaeiyan et al, if the plant biomass is less than 0.5 kg / m2, the vegetation effect can be ignored on the total backscatter coefficient (Das, 2008). In hot season, when the dehydration was high,

vegetation is noticeably reduced and less correlated with backscatter. Thus, it was proved that C band was affected by vegetation. In the studied area, the effect of vegetation was eliminated due to a variety of vegetation and its effects on backscatter.

4.3. Distribution of backscatter in time-spatial dimension

The normalized total backscatter was shown in 15 meters pixels during the study period. As seen, the total backscatter was affected by vegetation area. It should be noticed that the backscatter is obtained from the northern, northeastern and western parts of the region Figure 8, where there were more vegetation and thus more soil moisture (Mesri, 1392: 3).

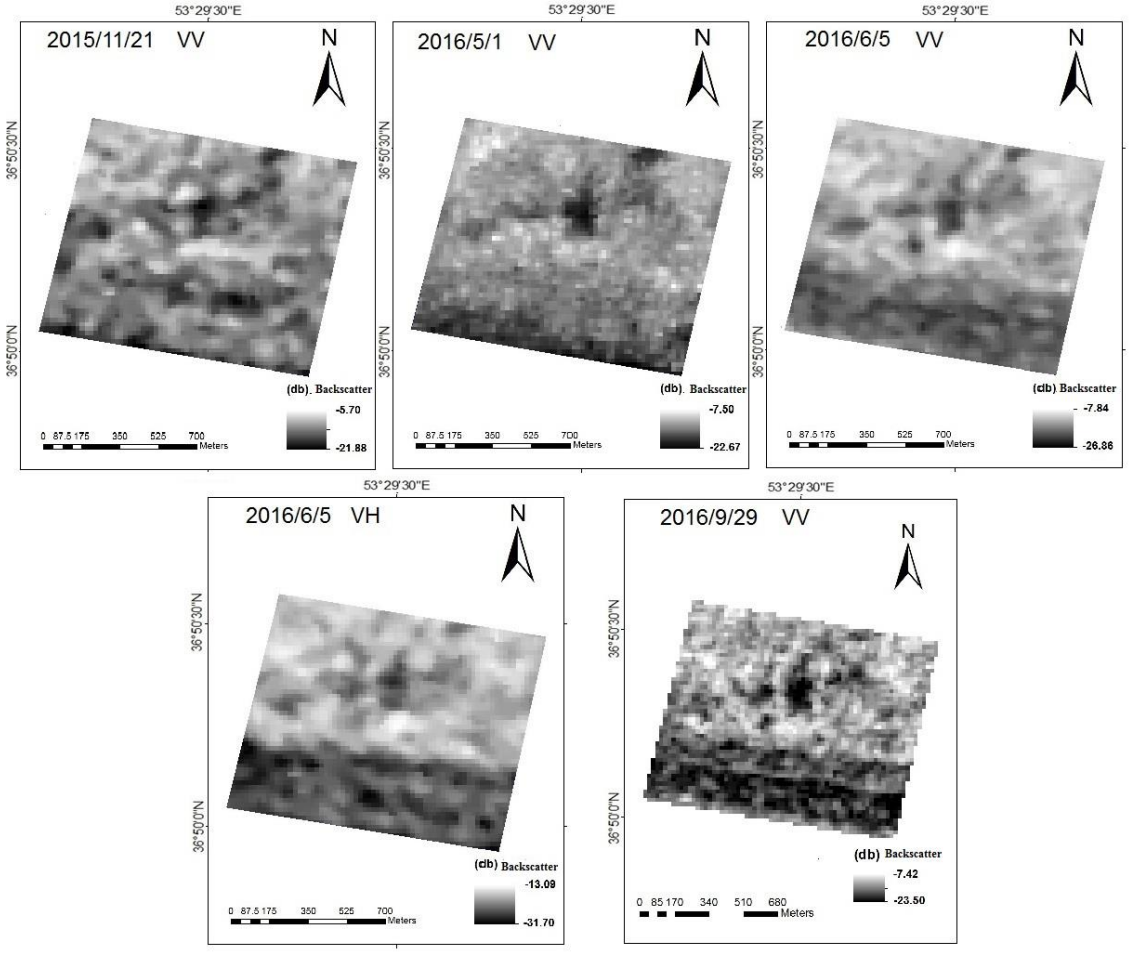

Fig. 7. Time-spatial distribution of the total backscatter (1 * 1 km).

4.4. Precision testing

Based on the results, the R^2 value was between 0.72 and 0.82, as well as RMSE between 1.75 and 0.35. The RMSE value was approximately dependent on the month or season of the year. In other words, in the low rainfall season, RMSE is somewhat diminished, as the effect of vegetation on backscatter. While Babaian et al. calculated 0.68 for R^2 based on surface soil moisture with ASAR images and HH polarization, the current research results in the VH and VV polarization, were above

0.70%. In addition, Salon et al. calculated moisture content using C-band with HH and VV polarization then reached to R^2 coefficients equal to 0.77, 0.81, and 0.88, which was approximately the same as this research.
In general, region vegetation diversity was very crucial and determined the accuracy of R2 coefficient. In the study of Nazari Aghdam, with satellite optic data, there was a high correlation between soil moisture content and NDVI. Therefore, in this study, there were no need for images in visible wavelengths. In Khan mohammadi research, vegetation indices such as NDVI, NDMI and LST employed using MODIS satellite data to extract soil moisture content. Although measuring soil moisture in Khan mohammadi research definitely affected by vegetation areas; its precision was not good enough compared to this research. According to Figure (8), the moisture content of the whole Miyankale Peninsula was mapped based on each image on SAR sensor.

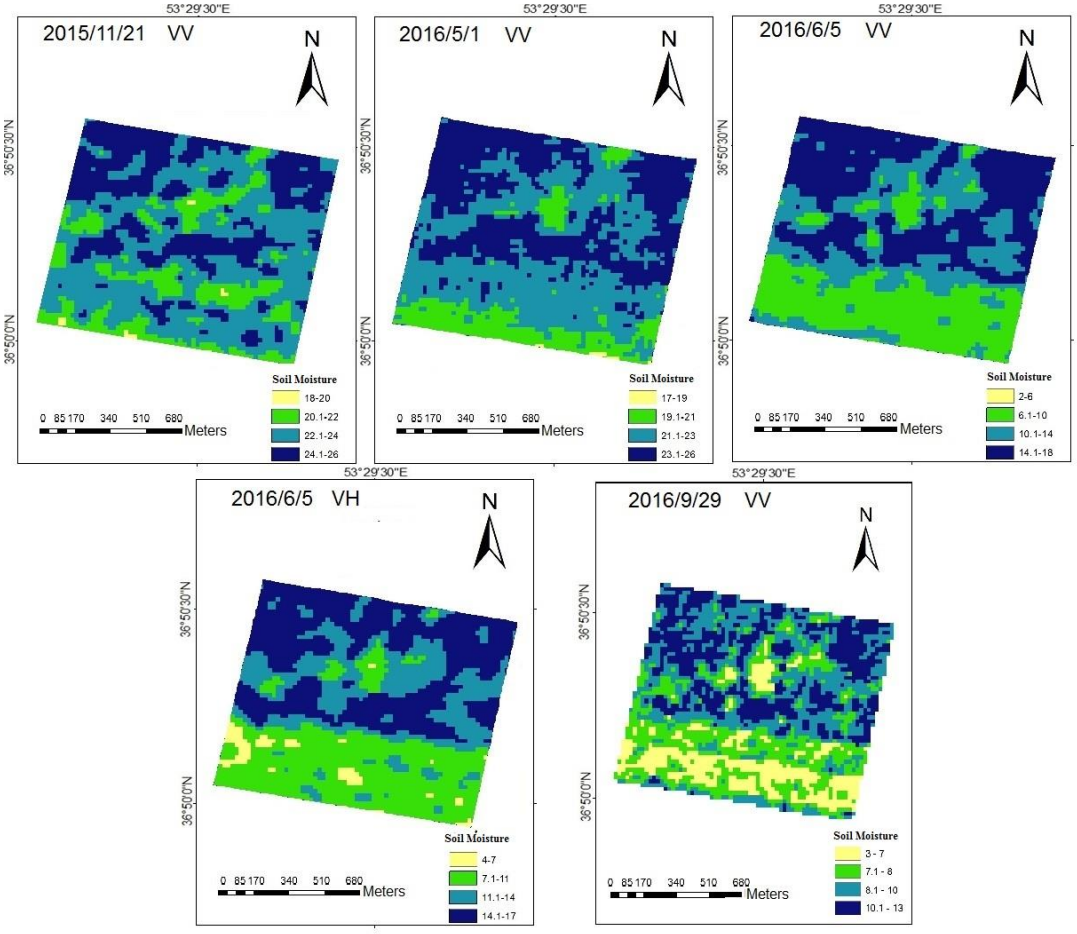

Fig. 8. Time-Spatial distribution of soil moisture content 1 * 1 km.

5. Conclusion

In this research, a simple experimental model proposed which was based on the backscatter data in GM mode of the Sentinel Satellite. The time-spatial model was proposed to retrieve, monitor, and mapping soil moisture of the earth surface. This regression model estimated soil moisture content in the study area through the R2 coefficient and RMSE calculations. The results of the evaluation and validation of the model showed that there is little difference between the soil moisture content and the

measured values. Due to the lack of coherent data of soil moisture in the country Iran, especially in crucial agricultural sites, employing the SAR data from the GM model would be an effective novel method. In this regard, it is recommended to use long-wavelength bands for vegetation areas.

REFERENCES

Babayan, A., Homaei, M., and Nowruz, AS., (2013). Estimation of Surface Soil Moisture Using ENVISAT / ASAR Radar Images, *Journal of Water Research in Agriculture*, 27 (4), pp. 622-611. https://journals.iau.ir/article_665927_04b010dd7d0c510562fb66445c43e278.pdf

Behyar, m.b., (2014). Evaluation of Soil Moisture in Isfahan Province by AMSR-E, *Geographic Quarterly Journal*, 29 (112), pp. 8-1. DOI:10.2136/vzj2013.05.0093

Khan mohammadi, F., Homaei, M., and Nowruz, AS a., (2014). Estimation of Soil Moisture Using Vegetation Indices and Soil Temperature and Normalized Moisture Index Using MODIS Images, *Journal of Soil and Water Resources Conservation*, 4 (2), pp. 9-1. DOI: 20.1001.1.22517480.1393.4.2.4.5

Mesri, a. Kamkarrowhani, A. Arab Amiri, A (2013): Determination of Soil Moisture Content Using GPR Method and Comparison of Results with Laboratory Results, Case Study: Shahroud University Agricultural University Campus, 8th Conference of Engineering and Environmental Geology of Iran, Ferdowsi University of Mashhad, p. 7. https://www.sid.ir/paper/852261/fa

Mirmazlomi, S.M. Sahebi, M. R., (2014): Estimation of soil moisture content using SAR data with emphasis on surface re-diffusion models, PhD thesis of Civil Engineering, Mapping Engineering, Khaje Nasir-e-Din Tusi University of Technology, Pages 110. https://elmnet.ir/doc/10787550-32212

Norozi Aghdam, A., Behbahani, M.R., Rahimi Khob, ., Aghighi, H., (2008): Surface Soil Moisture Model Using NDVI Index (Case Study: Rangelands of Khorasan Province), Journal of Environmental Studies, 2006, No. 48, Pages 127-136, DOI: 20.1001.1.10258620.1387.34.48.12.1

Altese .E, Bolognani .O, Mancini .M, and Troch, P.A, (1996): Retrieving soil moisture over bare soil from ERS1 Synthetic Aperture Radar data: sensitivity analysis based on theoretical surface scattering model and field data, Water Resources Research J, 32: 653-661. DOI: 10.1029/95WR03638

Baghdadi. N, Aubert. M and Zribi. M, (2012): Use of TerraSAR-X data to retrieve soil moisture over bare soil agricultural fields. IEEE Geoscience and Remote Sensing Letters, 9: 3-12. https://hal.science/hal-00704953/document

Balik Sanli. F, Kurucu. Y, Tolga Esetlili. M, Abdikan. S, (2008): Soil Moisture Estimation from Radarsat -1, Asar and Palsar Data In Agricultural Fields Of Menemen Plane Of Western Turkey. The International Archives of the Photogrammetry, Remote Sensing and Spatial Information Sciences, Vol. XXXVII. Part B7. https://www.isprs.org/proceedings/xxxvii/congress/7_pdf/2_wg-vii-2/02.pdf

Brocca. L.S, Hasenauer. T, Lacava. F, Melone. T, Moramarco. W, Wagner. W, Dorigo. P, Matgen. J, Martínez-Fernández. P, Llorens. J, Latron. C and Martin. M, (2011): Soil moisture estimation through ASCAT and AMSR-E sensors: an intercomparison and validation study across Europe, Remote Sensing of Environment J., 115:3390–3408. DOI:10.1016/j.rse.2011.08.003

Das. N.N, Mohanty. B.P and Njoku. E.G, (2008): A Markov chain Monte Carlo algorithm for upscaled SVAT modeling to evaluate sattelite-based soil moisture measurements,Water Resources Research, 44:W05416. DOI:10.1029/2007WR006472

Entekhabi. D, Nakamura. H and Njoku. E.G, (1994): Solving the inverse problem for soil moisture and temperature profiles by the sequential assimilation of multifrequency remotely sensed observations. IEEE Trans. Geosci, Remote Sensing, 32: 438-448. **DOI:** 10.1109/36.295058

Kolassa. J, Gentine. P, Prigent. C, Aires. F, (2016): Soil moisture retrieval from AMSR-E and ASCAT microwave observation synergy. Part 1: Satellite data analysis, Remote Sensing of Environment, 173: 1–14. DOI:10.1016/j.rse.2015.11.011

Lievens, H. Martens, B. Verhoest, N.E.C. Hahn, S. Reichle, R.H. Miralles, D.G. (2017): Assimilation of global radar backscatter and radiometer brightness temperature observations to improve soil moisture and land evaporation estimates, Remote Sensing of Environment 189: 194–210. https://doi.org/10.1016/j.rse.2016.11.022

Lievens. H and Verhoest. N.E.C., (2012): Spatial and temporal soil moisture estimation from RADARSAT-2 imagery over Flevoland, The Netherlands, Journal of Hydrology, 456: 44-56. DOI:10.1016/j.jhydrol.2012.06.013

Mecklenburg. S, Drusch. M, Kaleschke. L, Rodriguez-Fernandez. N, Reul. N, Kerr.Y, Font. J, Martin-Neira. M, Oliva. R, Daganzo-Eusebio. E, Grant. J.P, Sabia. R, Macelloni. G, Rautiainen. K, Fauste. J, de Rosnay. P, Munoz-Sabater. J, Verhoest. N, Lievens. H, Delwart. S, Crapolicchio. R, de la Fuente. A, Kornberg. M, (2015): ESA's Soil Moisture and Ocean Salinity mission: From science tooperational applications, Remote Sensing of Environment. RSE-09658: No of Pages 16. DOI: 10.1016/j.rse.2015.12.025

Minchella, Andrea, (2016): SNAP Sentinel-1 in a Nutshell, – "ESA SNAP-Sentinel-1 Training Course"Satellite Applications Catapult - Electron Building, Harwell, Oxf. https://www.academia.edu/26646467/SNAP_Sentinel_1_in_a_Nutshell

Moran. M. S, McElroy. Stephen, Watts. Joseph M and Peters-Lidard. Christa D, (2005): Radar Remote Sensing for Estimation of Surface Soil Moisture at the Watershed Scale, Radar Remote Sensing for Estimation of Surface Soil Moisture at The Watershed Scale, p:17. https://www.researchgate.net/publication/255606424_Radar_Remote_Sensing_for_Estimation_of_Surface_Soil_Moisture_at_the_Watershed_Scale

Sanli. F.B, Kurucu. Y, Esetlili. M.T and Abdikana. S, (2008): Soil moisture estimation from RADARSAT-1, ASAR and PALSAR data in agricultural fiels of Menemen plain of western Turkey.The International Archives of the Photogrammetry, Remote Sensing and Spatial Information Sciences. Part B7, Beijing. https://www.researchgate.net/publication/232269197_SOIL_MOISTURE_ESTIMATION_FROM_RADARSAT_-1_ASAR_AND_PALSAR_DATA_IN_AGRICULTURAL_FIELDS_OF_MENEMEN_PLANE_OF_WESTERN_TURKEY

Thain. C, Barstow. R, Ramsbottom. D, Lim. P, Wong. T, (2011). Sentinel-1Product Specification, Ref: S1-RS-MDA-52-744, Issue/Revision: 2/2. https://journals.iau.ir/article_665927_04b010dd7d0c510562fb66445c43e278.pdf